ELM pacing with high frequency multi-species impurity granule injection in NSTX-U H-Mode discharges

R. Lunsford, A. Bortolon, A.L. Roquemore, D.K. Mansfield, M.A. Jaworski, R. Kaita, R. Maingi, A. Nagy and the NSTX-U team

Email: rlunsfor@pppl.gov
Princeton Plasma Physics Laboratory, 100 Stellarator Rd, Princeton, NJ 08540 USA

We report on ELM triggering and pacing experiments in NSTX-U, including comparisons to pellet ablation models. The ability to control Edge Localized Modes(ELMs) is required for successful operation of next generation plasma devices such as ITER. For discharges with a naturally low ELM frequency, on the order of a few Hertz, the impurity ejection provided by the ELMs is projected to be insufficient to control the buildup of impurities within the plasma core. To maintain a low Z_{eff}, the period between the ELMs must be smaller than the edge to core diffusion times of the sputtered divertor and first wall material. During the hydrogen/helium operational phase of ITER, the intrinsic ELM frequency is anticipated to be too low to provide sufficient impurity exhaust, and must be augmented through one or more techniques[1]. As the plasma current is increased, the spatial footprint of the energy exhausted to the plasma facing components by ELMs narrows; at some point, the unmitigated peak heat flux can exceed material integrity limits. Previous experiments[2] have demonstrated that there is an inverse relationship between the frequency of the triggered ELM and the peak heat flux contained within the mode. Thus to generate the required mitigation, a rapid triggering of ELMs, also called "pacing", is employed to reduce the peak heat flux. While recent results have called into question the efficacy of pacing in metal walled tokamaks[3], ELM pacing is one of a few baseline ELM heat flux mitigation strategies for ITER.

At NSTX-U multiple sizes and types of solid impurity granules are injected into the low field side of the plasma to determine their ELM triggering and pacing capability. Examining the penetration depths, mass deposition locations, and ELM triggering efficiencies of sub-mm lithium, boron carbide (B_4C) and carbon granules, we can assess the optimal size and composition for minimally perturbative ELM triggering. The solid granules are horizontally propelled into the plasma edge by means of a rapidly rotating dual bladed turbine impeller as described in [4]. The injector is capable of frequencies up to 500 Hz, with a maximum injection velocity of approximately 150 m/sec. Rapid electron heat conduction along the magnetic field lines causes the outer layer of the granule to rapidly ablate (Figure 1). The ablatant then forms a dense neutral cloud around the granule, shielding it from the surrounding plasma. Further heat input is absorbed by the neutral cloud, resulting in an ionization of the ablatant material that is conducted away from the granule along field lines at ion acoustic speed. This quasi-stasis of granule and neutral cloud is maintained until the granule can no longer replace the ablatant material lost to ionization. The mass deposition of these granules into the edge of the discharge leads to a peaking of the localized plasma pressure, and the creation of an overdense flux tube which becomes 3-D ballooning unstable, resulting in an ELM.

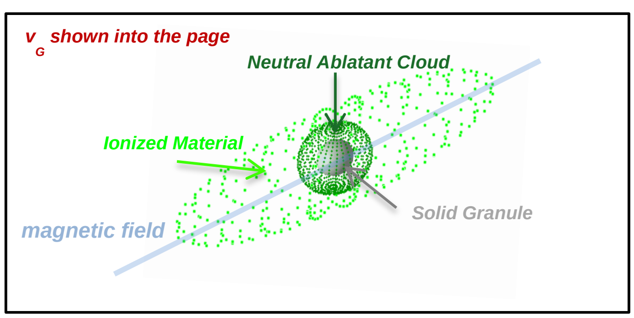

Figure 1: Ablation of an injected solid granule.

The ablation rates of the injected granules depend upon their mass densities and sublimation energy, leading to differing penetration depths and mass deposition locations for similar injection characteristics (i.e. granule size and injection velocity). By utilizing a neutral gas shielding model[5], benchmarked with lithium granule ablation experiments performed on DIII-D[4], the pedestal atomic deposition characteristics for the three different species of granule are projected for NSTX-U plasma edge characteristics. As shown in the upper panel of Figure 2, variations in the penetration depths of injected granules can range from 10 cm for lithium to 30 cm for the same size carbon granule.

Altering the injection velocity of the granule, presented in the lower three intensity graphs in Figure 2, can modify the mass deposition location, allowing further tuning of ELM triggering. By reducing the rotation speed of the impeller, the peak mass deposition location is translated closer to the top of the pedestal. At this location the pressure profile generated by the granule can be added to the preexisting pedestal pressure gradient, leading to a set of characteristics advantageous for ELM triggering while affecting a minimal perturbation to the core plasma. However, the reduced impeller speed will result in a lower granule injection frequency, reducing in principle the peak heat flux mitigation factor.

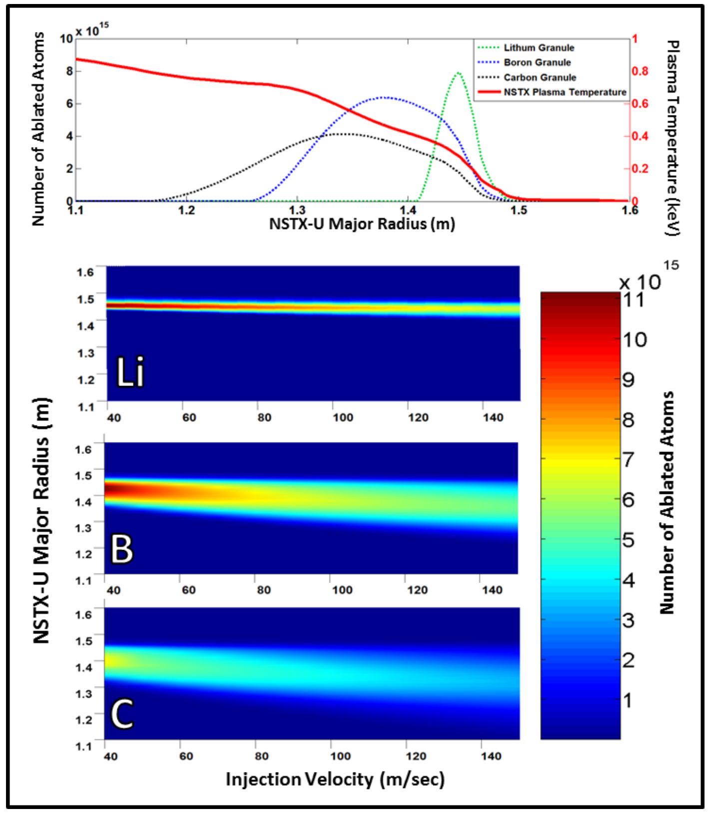

Figure 2: Mass deposition location for injected granules of differing species. The top panel displays the ablatant deposition for three 500 micron granules injected at 100 m/sec. The bottom three panels illustrate the variation in mass deposition location for alternate injection velocities. In these graphs the granule injection direction is from top to bottom.

Using multiple high-speed cameras to precisely track the granule injections and monitor the ablation duration and penetration depths in NSTX-U, a fractional mass deposition location can be extrapolated. The ELM seeded by granule injection at the discharge midplane is field line mapped to the divertor. Fast infrared camera measurements are used to characterize the variations between triggered ELMs and the inter-ELM period. In addition comparisons are also made between stimulated and spontaneously occurring ELMs. These measurements provide a comparison of the ELM peak heat flux mitigation factor, as well as variations in the ELM footprint due to the triggering mechanism. The results of ELM pacing and comparisons with the constructed ablation model in NSTX-U will be reported.

This work supported by US Department of Energy Contract No. DE-AC02-09CH11466

[1] A. Loarte et al., Nucl. Fusion **54** (2014) 033007
[2] L.R. Baylor et al., Phys Rev Lett. **110** (2013) 245001
[3] P.T. Lang, et al.," Nucl. Fusion **53** (2013) 073010
[4] A. Bortolon et al., Submitted to Nucl. Fusion NF-100993(2016)
[5] P.B. Parks et al., Nucl. Fusion **34** No. 3 (1994) 417